IEEE Access
Multidisciplinary | Rapid Review | Open Access Journal

Received December 5, 2019, accepted December 21, 2019, date of publication December 27, 2019, date of current version April 7, 2020.

Digital Object Identifier 10.1109/ACCESS.2019.2962749

Modulation Format Identification Based on an Improved RBF Neural Network Trained With Asynchronous Amplitude Histogram

SIDA LI, JING ZHOU, ZHIPING HUANG, AND XIAOYONG SUN
College of Intelligent Science, National University of Defense Technology, Changsha 410073, China

Corresponding author: Jing Zhou (zhou.jing@nudt.edu.cn)

This work was supported in part by the Frontier Science and Technology Innovation Project, in part by the National Key Research and Development Program under Grant 2016QY11W2003, in part by the Natural Science Foundation of Hunan Province under Grant 2018JJ3607, in part by the Natural Science Foundation of China under Grant 51575517, and in part by the National Technology Foundation Project under Grant 181GF22006.

ABSTRACT This paper proposed a method of modulation format identification using Radial Basis Function Artificial Neural Network (RBF-ANN) trained with Asynchronous Amplitude Histograms (AAHs). Compare with the traditional RBF-ANN, the proposed method is improved by applying Expectation Maximization (EM), which takes advantage of the statistical feature of AAHs, to select center vector for radial basis function. Assuming distribution of each bin in AAH as Gaussian mixture model (GMM), the mean values of the model can be exploited as the center vector which obtained using EM. This approach ensures that the center vector is unbiased and optimal. The center vector is implemented to RBF-ANN to identify different modulation formats. Numerical simulation results demonstrated that identification accuracy was about 99% for three commonly-used modulation formats within the OSNR between $40 \sim 10$dB. And the CD tolerance was 1000ps/nm. In comparison, former center vector selection approaches include K-means and random selection were applied. The result showed that the EM method improved the identification accuracy by 2% to 4% when OSNR $=$ 10dB and CD $=$ 100ps/nm. Owing to its excellent performance, this method can be employed in the next generation optical transport network for auto-adaption modulation format identification.

INDEX TERMS Modulation format identification, artificial neural network, asynchronous amplitude histogram, expectation maximization.

I. INTRODUCTION

The increasing demands of data bandwidth and line rate in modern information society have motivated the upgrading of optical networks. To fulfill need of massive data transmission, optical transmission techniques such as single-mode fiber, single-frequency laser, Erbium Doped Fiber Amplifier (EDFA), Wavelength Division Multiplexing (WDM) and advanced modulation scheme develop rapidly, making the transmission capacity nearly catching the limits specified by Shannon's theorem. To tackle this challenge, heterogeneous optical networks have gained significant attention over the past few years which may lead to the network architectures becoming more dynamic, complex, and transparent in nature. The growth of heterogeneous optical networks brings opportunities and challenges to the performance monitoring and management technology of optical communication networks. In order to realize the next generation dynamic reconfigurable optical network, it is necessary to monitor the important parameters, isolate faults in time and optimize the processing to ensure the transmission quality of the network. Hence, it is indispensable to have appropriate optical performance monitoring (OPM) technology dedicating for enhancing quality of service (QoS) and non-mistake transformation. OPM technology includes optical signal-to-noise ratio (OSNR) estimation, modulation formats identification(MFI), symbol rate estimation and others fiber link crucial injuries monitoring, to name a few, chromatic dispersion (CD), polarization mode dispersion (PMD) and nonliner interferences. Network operators need the integration of

The associate editor coordinating the review of this manuscript and approving it for publication was Zhen Ren.

OPM and network management urgently. In 10G/40G single polarization intensity modulation optical networks, there are equipment providers delivering service to long-haul transmission system using OPM module which can provide real-time power, wavelength and OSNR monitoring. For optical network, OPM can enhance scalability and flexibility, guarantee the quality of transmission service, provide protection and recovery. Currently Alcatel-Lucent, Huawei and Beacon are all carrying out relevant research. In terms of network management, optical performance monitoring and real-time knowledge of the quality of optical network transmission are the basic basis for operators to ensure the quality of their services. Accordingly, OPM is not only a concernment for the current optical network, but also significant for the new generation of optical network. So far, many efficient OPM schemes are proposed by researchers. The mathematical foundations of basic Machine Learning techniques for OPM was described in system by Khan *et al.* [1]. In paper [2], joint OPM and modulation format/Bit-Rate identification approaches based on CNN was proposed. Paper [3] illustrated the experimental demonstration of simultaneous MFI and symbol rate identification. Optical spectrum based OSNR monitoring approach was demonstrated in paper [4]. Xu proposed a joint scheme of dynamic polarization demultiplexing and PMD compensation in paper [5]. Modulation Format Identification is a technology to acquire the modulation information of the transmission signal, obtain the heterogeneous transmission service information and provide important references for allocating the optimal transmission in the middle node of the network.

Modulation format Identification has gained significant attention over the past decades. Signals with different modulation formats have different anti-injuries capacities on transmission links. It is foreseeable that future optical network will transmit signals with different modulation formats. To support this heterogeneity, OPM technology is expected to have modulation format identification function to identify different modulation formats. MFI techniques for optical network include identification based on artificial neural networks (ANN) [6], [7], K-means-based constellation diagram identification technique [8], stokes space-based methods [9], [10] and newly proposed nonlinear power transformation [11], etc. K-means-based constellation diagram identification need ideal constellation diagrams which is hard to acquire under practical circumstances. Stokes-based methods describe the polarization of light beam with four parameters and signal modulation information can be reflected well in Stokes-space. To calculate these parameters, synchronize sampling data is required which could be hampered by lacking of high speed sampling equipment. The nonlinear power transformation technique is based on Fast Fourier Transformation (FFT) and higher-order spectral. The drawback is that an artificial choice of peak-to-average power ratio (PAPR) threshold is needed. In contrast, ANN shows great flexibility and efficiency because of its learning ability. By simulating the learning process of humans' brain, ANN make reasonable judgements and decisions for complex problems based on the learned knowledge and experiences. This feature enhances ANN's robustness in function approximation, classification and identification, especially when supported with abundant data set.

ANNs have developed various branches with the time passing by. Many of ANNs have been employed for MFI in OPM, namely Backpropagation (BP) Network, Radial Basis Function Artificial Neural Network (RBF-ANN) and Deep Learning Methods [12]. Conventional BP bas two drawbacks: 1). the convergence speed of is slow; 2).easy to get stuck at local minima. Deep learning Methods improve performance by increasing network complexity with at least eight layers in the net. To ensure the real-time performance of the deep learning methods, more and better hardware support are required. For this reason, Deep learning Methods are resources consuming which are intensely limited in OPM systems, especially in embedded processing system for OPM. In contrast, RBF-ANN has three-layer perceptron structure and partial response feature, which saves hardware resources than deep learning and performs better in classification ability and learning speed than BP. RBF network with PCA had been used for center selection, with application to aerodynamic modeling of airfoils by Zhang *et al.* [13]. Kou used RBF as a component for novel Wiener model to identify and model the nonlinear dynamic systems with strong nonlinearity [14]. In a nutshell, among machine leaning methods, RBF-ANN is more efficient and resources saving for OPM system.

Asynchronous Amplitude Histogram (AAH) is an efficient technology for OPM system because of its low cost and bit rate transparency. In previous work, RBF-ANN trained with eye-diagram had been proved to be of limited practical use in OPM [15]. The drawback of this approach is that eye-diagram will deteriorate when lacking of clock recovery and compensation for transmission impairments. In spite of eye-diagram, AAH is a conventional approach that contains features of signals, and in contrast, eliminates the disadvantages may occur among its counterparts. Recently, it has been used for symbol rate identification and shows its advantage in avoiding usage of expensive sampling hardware [16]. But it is worth noting that the statistical characteristics of AAH is not fully analyzed and exploited. In our work, statistical method (Expectation Maximization) is implemented to analysis AAHs to make better use of the statistical characteristics.

In this paper we propose a resource saving and precise MFI technique based on the EM improved RBF-ANN trained with AAHs. AAHs are applied to train the RBF-ANN to identify different modulation formats in optical network. The RBF-ANN is improved by using Expectation Maximization to select center vector. Assuming distribution of each bin in AAH as Gaussian mixture model (GMM), the average values of the model can be applied as the center vector which can be obtained using EM. Numerical simulations have been performed for three commonly used signal polarization modulation formats: Non-Return to Zero (NRZ) 16 quadrature amplitude modulation (16-QAM), NRZ binary phase

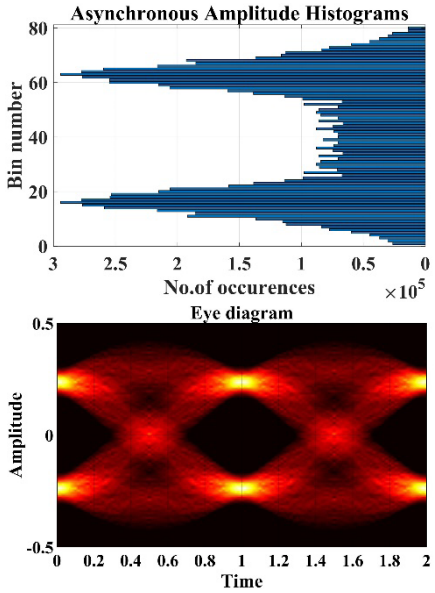

FIGURE 1. Eye diagram and asynchronous amplitude histogram for QPSK signal.

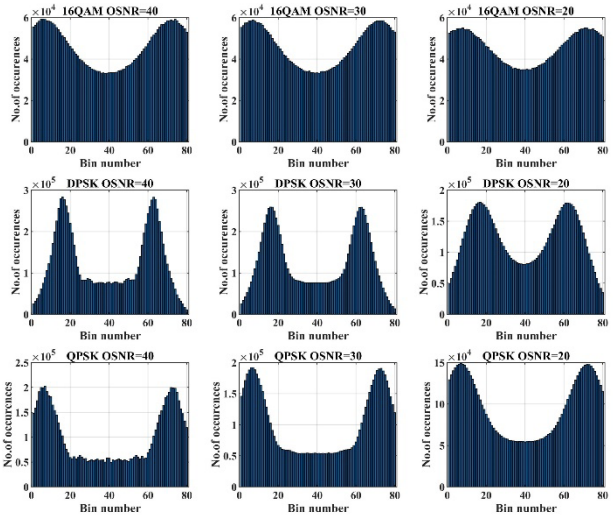

FIGURE 2. AAHs obtained from NRZ-16QAM (top panel), NRZ-DPSK (middle panel) and NRZ-QPSK (bottom panel) signals with different OSNRs (40dB, 30dB and 20dB).

shift keying and NRZ quaternary phase shift keying to test algorithms' reliability. The simulations results demonstrate that the new method can successfully recognize different modulation formats with OSNR between 40dB to 10dB. And CD and PMD tolerance is also evaluated by experiment simulation. Further simulation is implemented and proved that EM method is better than existing center vector selection methods for RBF-ANN in MFI.

The paper is organized as follows. In Section 2 the principle of the AAH, RBF-ANN and improved center vector method (EM) is described. Section 3 details the simulation setup to validate the proposed method. Section 4 presents the results and discussion. Finally, conclusions are stated in Section 5.

II. PRINCIPLE

A. PRINCIPLE OF ASYNCHRONOUS AMPLITUDE HISTOGRAM

Asynchronous Amplitude Histogram is an efficient technology for OPM system because of its low cost and bit rate transparency. Eye diagram is synchronous amplitude diagram from a full bit period signal. When lacking of clock information, asynchronous sampling has to be applied which's amplitude diagram is random sampling from a full bit period signal. In another word, we can obtain the pulse amplitude distribution map when there are overwhelming sampling points. Fig.1 shows the eye diagram and AAH for QPSK signal. AAH is an efficient technology for OPM system because of its low cost and bit rate transparency. And AAH can reflect the distinct features of different modulation formats signals [17]. Fig.2 shows AAHs of signals with different modulation formats in different OSNRs. As shown in Fig.2, the amplitude distributions of varies modulation formats have significant differences, to name a few, the maximum value, the minimum value, the position and number of peaks and the slope between bins, which means we can use these differences as the features to identify modulation formats. Hereby, ANN is implemented for MFI.

AAH can be applied to evaluate the quality of signals and is highly sensitive to OSNR and transmission impairments such as CD and PMD. It has also been used to monitor the OSNR of PDM-QPSK signal systems [18]. Literature [19] demonstrated in both theory and experiment that asynchronous amplitude histograms can be exploited to monitor CD and OSNR. In our work, AAH is used as the input of the neuron network to identify modulation formats.

B. STRUCTURE OF RBF-ANN

ANNs are neuroscience-inspired computational tools which are trained by input-output data to generate a desired mapping from an input stimulus to the targeted output [6]. The structure of RBF-ANN has been well laid out in many recent work [20], [21]. In the proposed technique, the AAHs are used as inputs which are represented by M × 1 vectors $\mathbf{x}$. In the training phase of ANN, each input vector $\mathbf{x}$ has a corresponding N × 1 binary vector $\mathbf{y}$ with only one non-zero element, indicating the signal modulation format type. The number of hidden layer neurons is setup between 4-10 and optimized by applying simulation. Gaussian kernel function ϕ is selected as the radial basis function in hidden layer. Fig.3 illustrates the structure of RBF-ANN model built for ours MFI purpose.

The model can be represented as

$$y_j = \sum_{i=1}^{N} w_{ij}\phi\left(\|\mathbf{x}-\mathbf{u_i}\|\right), \quad (j = 1, \ldots, p)$$
$$\text{where } \|\mathbf{x}\|^2 = \sum_{k=1}^{m} x_k^2 \tag{1}$$

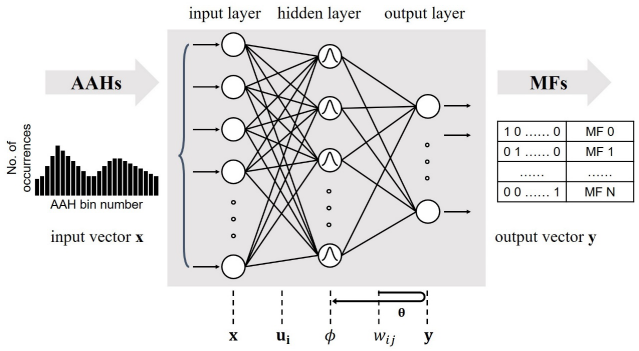

FIGURE 3. Structure of modulation formats identification model using RBF-ANN trained with AAHs.

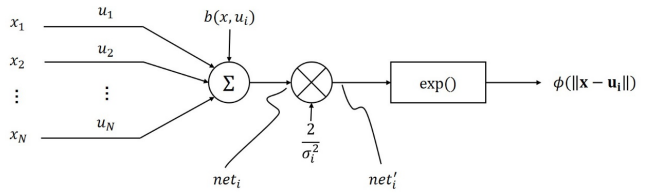

FIGURE 4. structure of hidden layer of RBF-ANN.

where $\mathbf{y}$ is the output vector, $\mathbf{x}$ is the input vector, ϕ is the gaussian kernel function, $\mathbf{u_i}$ is the $i'th$ center vector and w_{ij} is the weight between hidden layer and output layer. In practical use, the center vector $\mathbf{u_i}$ is the AAHs of different the signal modulation format type with no transmission impairments. The weight w_{ij} is initialized to be random value and updated following least mean square (LMS) criterion.

To be specific, radial basis function takes the following form

$$\phi\left(\|\mathbf{x}-\mathbf{u_i}\|\right) = e^{-\frac{\|\mathbf{x}-\mathbf{u_i}\|^2}{\sigma_i^2}} \tag{2}$$

where σ is the standard deviation of center vector. Expansion index item of the radial basis Function, we have

$$\begin{aligned}\frac{\|\mathbf{x}-\mathbf{u_i}\|^2}{\sigma_i^2} &= \frac{1}{\sigma_i^2}\left(\mathbf{x}-\mathbf{u_i}\right)^T\left(\mathbf{x}-\mathbf{u_i}\right)\\ &= \frac{1}{\sigma_i^2}\left(\mathbf{x}^{\mathrm{T}}\mathbf{x}-\mathbf{x}^{\mathrm{T}}\mathbf{u_i}-\mathbf{u_i}^{\mathrm{T}}\mathbf{x}+\mathbf{u_i}^{\mathrm{T}}\mathbf{u_i}\right)\\ &= \frac{2}{\sigma_i^2}\left(\frac{\|\mathbf{x}\|^2+\|\mathbf{u_i}\|^2}{2}-\mathbf{u_i}^{\mathrm{T}}\mathbf{x}\right)\end{aligned} \tag{3}$$

Define bias $b\left(\mathbf{x},\mathbf{u_i}\right)$ as

$$b\left(\mathbf{x},\mathbf{u_i}\right) = -\frac{\|\mathbf{x}\|^2+\|\mathbf{u_i}\|^2}{2} \tag{4}$$

Combine with Eq.3 and Eq.4 we have

$$\phi\left(\|\mathbf{x}-\mathbf{u_i}\|\right) = e^{\frac{2}{\sigma_i^2}\left(\mathbf{u_i}^{\mathrm{T}}\mathbf{x}+b(\mathbf{x},\mathbf{u_i})\right)} \tag{5}$$

According to this equation, we can demonstrate the hidden layer neuron as Fig.4
where net_i and $net_i^{'}$ are the output vector of sum function and input of active function, respectively. The Eq.5 and

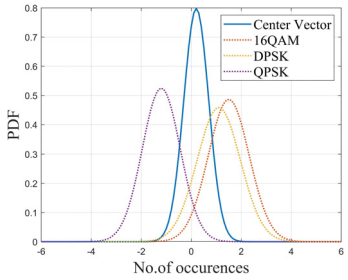

FIGURE 5. Distribution of AAH bins of center vector and different modulation formats.

Fig.4 illustrate the distinctions between BP neural network and RBF neural network: a). weights between input layer and hidden layer in RBF-ANN is depend on center vector; b). bias $b\left(\mathbf{x},\mathbf{u_i}\right)$ has automatic gain control function to outputs of hidden layer of RBF-ANN; c). input vector of active function $net_i^{'}$ is self-adaptive to width of RBF σ_i because of $net_i^{'} = 2net_i/\sigma_i^2$. These features decide selection of the pivotal parameters in RBF-ANN: center vector $\mathbf{u_i}$ and standard deviation of center vector σ.

Conventional approaches of center vector selection for RBF include K-means and random selection. K-means algorithm is widely used in selecting center vector. The fundament thought of K-means is searching for the minimum Euclidean distance between input vector and center vector. The center vector is initialized randomly and updates following

$$\mathrm{u}_i\left(n+1\right) = \mathrm{u}_i\left(n\right) + \eta\left\|\mathrm{x}\left(n\right) - \mathrm{u}_i\left(n\right)\right\| \tag{6}$$

where η is learning rate, normally 0.01.

Random selection algorithm is selecting center vector randomly.

The drawbacks of the existing center vector approaches include: a). priori information of the sampled signals is not used; b). the estimation is a biased estimate. For these reasons, K-means and random selection are not recommended in modulation format identification when AAHs is applied.

C. CENTER VECTOR SELECTION OF WITH EXPECTATION MAXIMIZATION (EM)

The AAH is a statistical methods in which each bin is a statistical value with unknown means and variances. The center vector selection problem comes down to finding a vector which's distribution parameters match the PDF of AAH bins for different modulation formats, as shown in Fig.5. This problem can be tackled by applying Expectation Maximization method which is elaborated in this section.

We assume the distribution of each bin in AAH as Gaussian mixture model (GMM). The mixed probability density function (PDF) can be represented as

$$\begin{aligned}p\left(x_i\right) &= \sum_{k=1}^{K} p\left(k\right) p\left(x_i \mid k\right)\\ &= \sum_{k=1}^{K} \pi_k N\left(x_i \mid u_k, \sum\nolimits_k\right), (i = 1, 2, \ldots, 80)\end{aligned} \tag{7}$$

where $p(x_i)$ is PDF of i^{th} bin of AAH, $p(x_i \mid k) = N(x_i \mid u_k, \sum_k)$ is PDF of k^{th} Gaussian model, also can be explained as probability of model generating x_i after k^{th} model is selected, $p(k) = \pi_k$ is weight of k^{th} Gaussian model, also called prior probability of selecting k^{th} model, we have $\sum_{k=1}^{K} \pi_k = 1$, u_k and $\sum_k$ are mean and covariance matrix of k^{th} model, respectively.

Based on the model, the center vector selection problem can be expressed as: estimating parameter group $\pi_1, \ldots, \pi_k; u_1, \ldots, u_k; \sum_1, \ldots, \sum_k$ of GMM PDF with given sample data $x = \{x_1, x_2, \ldots, x_N$ and order of GMM model m (determined by number of hidden layer neurons). Under this circumstance, Expectation Maximization (EM) is implemented to estimate PDF parameter group.

Firstly, we introduce an latent variable γ which is a k dimension binary random variable. In its k dimension, only one specific element has a value of 1, while the other elements have a value of 0. In fact, latent variables describe the probability of choosing the k^{th} Gauss model for each sampling. So, we have:

$$p(\gamma_k = 1) = \pi_k \tag{8}$$

Given a specific value of γ (i.e. knowing the Gaussian model which data is sampled from), it can be concluded that the conditional distribution of the sample y is a Gaussian distribution, which following:

$$p(y|\gamma_k = 1) = N(y|u_k, \sum\nolimits_k) \tag{9}$$

In fact, it is impossible to know the Gaussian model which the data is sampled from. So the probability of sample y is:

$$p(y) = \sum\nolimits_\gamma p(\gamma)\, p(y \mid \gamma) = \sum\nolimits_{k=1}^{K} \pi_k N\left(\mathrm{y} \mid u_k, \sum\nolimits_k\right) \tag{10}$$

The joint probability of sample set Y (n sample points) is:

$$\begin{aligned} \mathrm{L}(\mathrm{u}, \textstyle\sum, \pi) &= L(y_1, y_2 \ldots y_N; \mathrm{u}, \textstyle\sum, \pi) \\ &= \textstyle\prod_{n=1}^{N} p(y_n; \mathrm{u}, \sum, \pi) \\ &= \textstyle\prod_{n=1}^{N} \sum_{k=1}^{K} \pi_k N\left(\mathrm{y}_n \mid u_k, \sum_k\right) \end{aligned} \tag{11}$$

The logarithmic likelihood function is expressed as:

$$\ln \mathrm{L}(\mathrm{u}, \textstyle\sum, \pi) = \sum_{n=1}^{N} \ln \sum_{k=1}^{K} \pi_k N\left(\mathrm{y}_n \mid u_k, \sum_k\right) \tag{12}$$

We can get the parameters $\pi_1, \ldots, \pi_k; u_1, \ldots, u_k; \sum_1, \ldots, \sum_k$ of the model by deriving and letting the derivative be 0. Then, $u_1, \ldots, u_k$ are used as the center vector in the RBF-ANN.

The selection of standard deviation of center vector σ, also called the width of basis function, follows the function:

$$\sigma_i^2 = \frac{1}{N_i} \sum_{j=1}^{N_i} \left(x_i^j - u_i\right)^2, (i = 1, 2, \ldots, k) \tag{13}$$

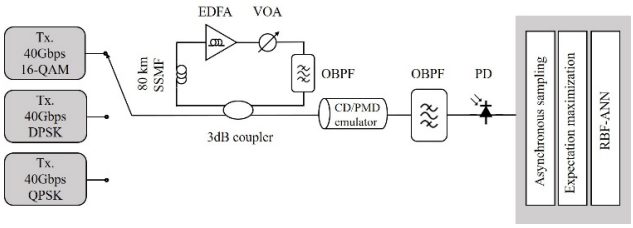

FIGURE 6. Simulation setup for MFI based on RBF-ANN trained with AAHs.

where σ_i^2 is the width of i^{th} bin of AAH, N_i is the number of data of i^{th} bin of AAH, u_i is the center vector generated from the EM method.

III. SIMULATION SETUP

To demonstrate the validity of the proposed MFI technique based on EM improved RBF-ANN trained with AAHs, numerical simulations are implemented using the software OptiSystem. Simulation is setup as shown in Fig.6.

Before simulation is set up, three modulation formats are chosen to test the proposed technology. Among all possible modulation formats, BPSK is widely recognized to have the best sensitivity, for which it is chosen as a reference [22]. In contrast, QPSK can be seen as two parallel BPSK. Thus, the sensitivity for QPSK is the same as that for BPSK. Moreover, with the development of coherent receiver, 16-QAM is applied for long-haul transmission at a line rate over 10Gbaud and high spectral efficiencies beyond 4 b/s/Hz [23]. These modulation formats are commonly used in optical transmission network, especially for long distance communication. On-Off Keying (OOK) is not within the consideration because it is relatively easy to recognize OOK signal in the time domain for its return to zero feature.

The simulation setup is shown in Fig.6. In Tx module, 40Gbps NRZ-16QAM,40Gbps NRZ-DPSK and 40Gbps NRZ-QPSK were generated using Mach–Zehnder modulators to modulate the symbols (generated by sequence generator and pulse generator) onto optical carrier. The center wavelength of optical carrier, generated by continuous wave (CW) laser, was 1550nm and its linewidth was 100kHz. The single polarization signals then transmitted through the optical channel. The optical signals were transmitted over a fiber recirculating loop comprising of an 80km span of standard single-mode fiber (SSMF), a variable optical attenuator (VOA), a EDFA and a 5nm bandwidth optical band-pass filter (OBPF) for equalizing channel power. The VOA was utilized to alter OSNRs of 16-QAM, DPSK and QPSK signals in the range of 10-40dB in approximately (initially 40dB). At the loop output, the CD/PMD emulator was applied to alter CD of the signal from 0 to 2,000ps/nm and Differential Group Delay (DGD) from 0ps to 10ps. The optical signals at the output of emulator unit were filtered by a 0.4 nm bandwidth OBPF to remove the redundant noise present in the signals. Then, the signal was detected by a photodetector (PD).

By asynchronous sampling, the training data and testing data were generated in form of AAHs. The training set swiped

TABLE 1. Estimation accuracies of the proposed MFI technique using the setup shown in Fig.7.

Actual Modulation Format	Identified Modulation Format		
	40Gbps NRZ-16QAM	40Gbps NRZ-DPSK	40Gbps NRZ-QPSK
40Gbps NRZ-16QAM	99.7%	-	-
40Gbps NRZ-DPSK	0.3%	99.9%	0.1%
40Gbps NRZ-QPSK	-	0.1%	99.9%

though OSNR values from 10 to 40 dB in steps of 5 dB, CD from 0 to 2000ps/nm in steps of 200ps/nm and DGD from 0 to 10ps in steps of 1ps. The testing data covered OSNR values from 10 to 40 dB in steps of 10 dB, CD from 0 to 2000ps/nm in steps of 500ps/nm and DGD from 0 to 10ps in steps of 2ps. The different OSNR, CD and DGD values in the training and testing sets ensure the robustness of the MFI. The number of training data was three times of the number of testing data. To be specific, 3000 training data and 1000 testing data under certain condition were generated for the simulation. After the data was sampled, expectation maximization was utilized to find center vectors from the training sets. These center vectors are used by RBF-ANN to identify different modulation formats.

IV. RESULTS AND DISCUSSION

In this chapter, result of the simulation is detailed. Fig. 7 depicts the output vectors y of the RBF-ANN trained with AAHs in response to 1000 input vectors x generated from the testing data set with OSNR = 30dB, CD = 100ps/nm, DGD = 5ps, number of hidden layer = 8. As we can see, three commonly-used modulation formats can be classified clearly as the output vectors show apparently differences. In detail, for Fig.7 (a), output vector is [0.54 0.25 0.21] in approximately. The first element (blue points) is over 0.5 which means the modulation format is estimated to be 16QAM to a great extent. In contrast, the output vectors when identifying DPSK and QPSK are about [0.05 0.58 0.37] and [0.10 0.34 0.56] (Fig.7 (b) and (c)), which means the technique perform well in identifying PSK, because the maximum elements in both vectors (red points and green points, respectively) are about 0.58 and 0.56. Table 1 summarizes MFI results for 1,000 test cases in testing data set. It is obvious from the table that the identification accuracy of three considered modulation formats is over 99%. Though the overall identification accuracy is acceptable, there are still some faults occurring as labeled by back circles in Fig.7. These faults occur in the overlap areas in the scatter plot.

To evaluate the effects of OSNR, CD and PMD on estimation accuracy for RBF-ANN trained with AAH, Fig.8 illustrates the identification accuracy changing in response to different OSNR, CD and DGD. For Fig.8 (a), it is evident that the identification accuracy goes down gradually for all three modulation formats with the drop down of OSNR. But overall accuracy is over 99% except for 16QAM (98.5% while

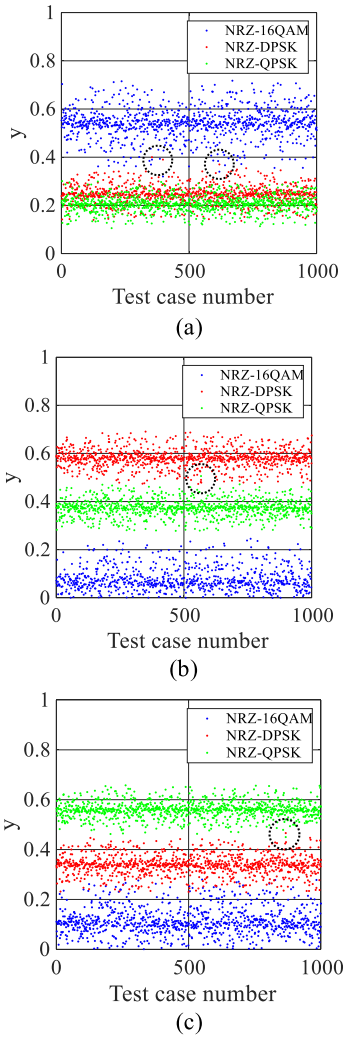

FIGURE 7. Elements of RBF-ANN output vectors y for (a)NRZ-16QAM,(b)NRZ-DPSK, and (c)NRZ-QPSK modulation formats in response to 1000 bin-count vectors x in the testing data set.

OSNR is 10dB), which means the RBF-ANN performs well under different OSNR. It is noteworthy that the curve of 16QAM falls down faster than its counterparts, which means the model is more robust while identifying PSK signal. For Fig.8 (b), before CD reach 1,000ps/nm, the identification accuracy reduces steadily with the increasing of CD. However, when CD grows to 1,500 and above, the identification accuracy for 16QAM drops down sharply under 80%. The identification accuracy for 16QAM dips to 42% when CD = 2,000ps/nm. These results prove that the tolerance for CD of proposed approach is 1,000ps/nm. In Fig.8(c), the accuracy drops down slowly with the increase of DGD. When DGD = 10ps, the accuracy is still over 99.5% for all three modulation formats. The result reveals that the estimation accuracy is slightly affected by DGD which means the PMD tolerance of proposed approach is good.

To optimize the parameters of the kernel function and improve the classification accuracy, simulation with different hidden layer neurons is setup. The number of hidden layer

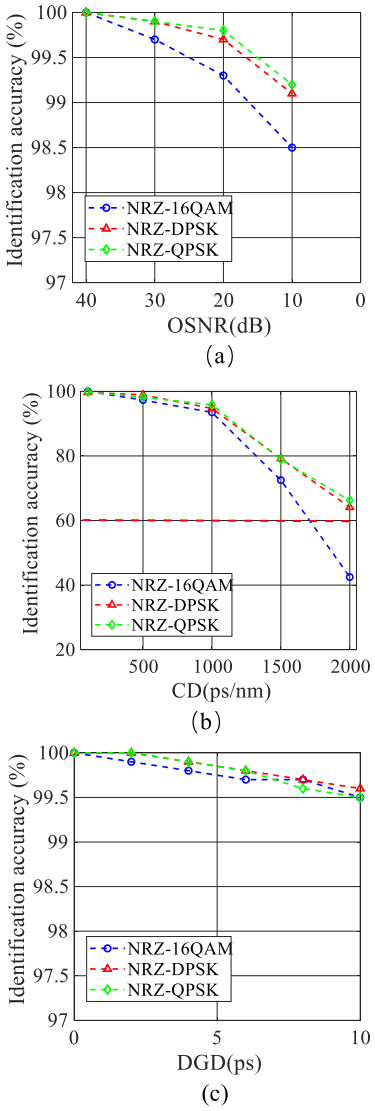

FIGURE 8. Effect of OSNR, CD and DGD on identification accuracy for proposed technique.

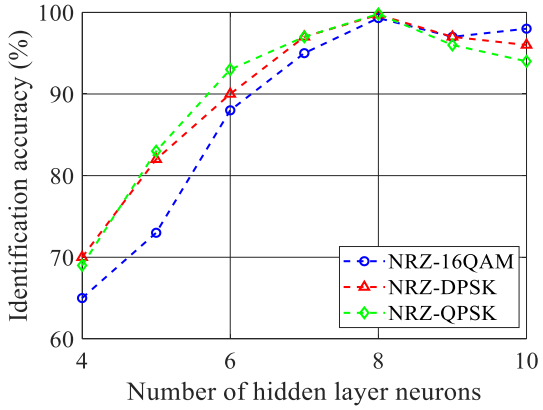

FIGURE 9. Identification accuracy of proposed technique with different number of hidden layer neurons (from 4 to 10) when OSNR = 20dB, CD = 100ps/nm and DGD = 5ps.

neurons is setup between 4-10 and optimized by applying simulations when OSNR = 20dB, CD = 100ps/nm and DGD = 5ps. Fig.9 show the identification accuracy when

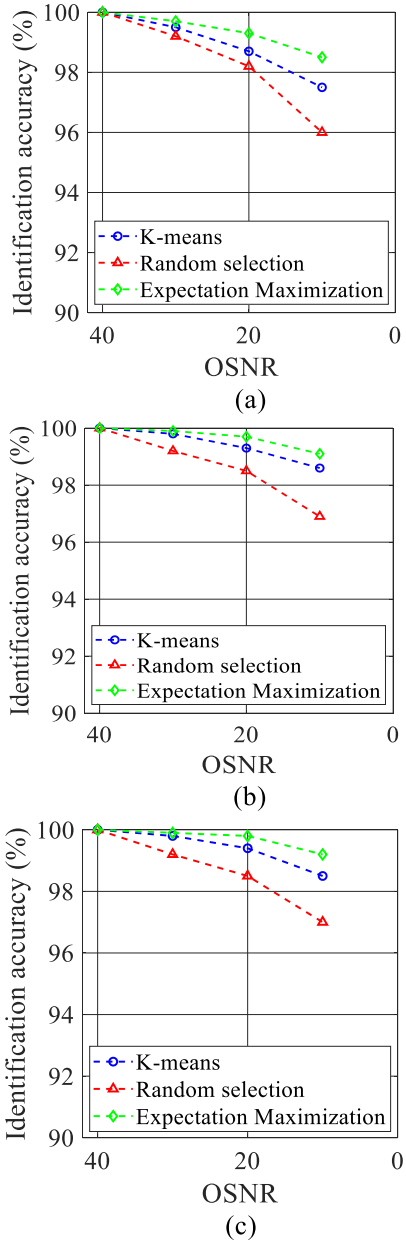

FIGURE 10. Effect of different center vector selection schemes on identification accuracy for 16QAM, DPSK and QPSK. The Fig.10 (a), (b) and (c) show identification accuracy for all methods applying for 16QAM, DPSK and QPSK respectively.

changing the number of hidden layer neurons. It is clear that the identification accuracy sharply grows up to about 99% with hidden layer increasing from 4 to 8. Then a slightly drop down occurs for DPSK and QPSK from 99% to about 95%. Likely, the accuracy for 16QAM signal fluctuates around 97%. Overall, when number of hidden layer neurons is 8, the model performance best for all three modulation formats.

To prove the effectiveness of the newly proposed center vector selection approach, we compared the identification accuracy of RBF-ANN with three different center vector selection methods. We assume the optimal number of hidden layer neurons is 8 for these schemes. As we can see in table 2,

TABLE 2. Estimation accuracies of three center vector selection schemes with different OSNR (CD = 100ps/nm, DGD = 5ps, Number of hidden layer neurons = 8).

OSNR (dB)	K-means			Random selection			Expectation Maximization		
	16QAM	DPSK	QPSK	16QAM	DPSK	QPSK	16QAM	DPSK	QPSK
40	100%	100%	100%	100%	100%	100%	100%	100%	100%
30	99.5%	99.8%	99.8%	99.2%	99.2%	99.2%	99.7%	99.9%	99.9%
20	98.7%	99.3%	99.4%	98.2%	98.5%	98.5%	99.3%	99.7%	99.8%
10	97.5%	98.6%	`98.5%	96.0%	96.9%	97.0%	98.5%	99.1%	99.2%

accuracy rate of all approaches can reach 100% when OSNR is 40dB and go down with the decline of OSNR for all three modulation formats. When OSNR is 10dB, the identification accuracy of K-means and Random selection based RBF-ANN see significant deterioration. In contrast, the EM methods can still successfully identify different modulation formats especially for DPSK and QPSK (99.1% and 99.2%). To clarify the result, Fig.10 depicts effect of different center vector selection schemes on identification accuracy for 16QAM, DPSK and QPSK.

To compare different center vector selection approaches' performance on each modulation formats, Fig.10 is made from Table 2. For Fig.10 (a), the identification rates of 16QAM go down with the deterioration of OSNR. Random selection method is significantly affected by OSNR with an average decreasing step of 1% and reach the lowest accuracy 96% among all panels. As for K-means, the drop step is about 0.6% which is moderate. In contrast, EM see slightly decrease with the average step 0.4%. It is clear that identification accuracy of EM is always the highest among three approaches when OSNR is the same. When OSNR is 10dB, the EM method improve the identification accuracy by 2% to 4%. The circumstances for the other modulation formats is almost the same. In summary, EM performs best among compared approaches and usable with the OSNR between 40dB-10dB.

The reasons of EM method outperforms other approaches can be conducted as the usage of priori information and its unbiasedness which has been illustrated in section II.

V. CONCLUSION

In this paper, we proposed a MFI technique for heterogeneous optical networks using EM improved RBF-ANN trained with AAH. The RBF-ANN is improved by optimizing the center vector selection scheme with Expectation Maximization. The principle of this approach was also presented and verified in the simulation. Numerical simulation results demonstrate that identification accuracy is about 99% for three commonly-used modulation formats within the OSNR between 40∼10dB. And the tolerance for CD is 1000ps/nm. In comparison, former center vector selection approaches including K-means and random selection were implemented. The result shows that the EM method improve the identification accuracy by 2% to 4% when OSNR is 10dB. To conclude, the new method can successfully recognize different modulation formats and promote the identification accuracy than the approaches compared. It is ideal for MFI in future heterogeneous optical networks.

REFERENCES

[1] F. N. Khan, Q. Fan, C. Lu, and A. P. T. Lau, "An optical communication's perspective on machine learning and its applications," *J. Lightw. Technol.*, vol. 37, no. 2, pp. 493–516, Jan. 15, 2019.

[2] X. Fan, Y. Xie, F. Ren, Y. Zhang, X. Huang, W. Chen, T. Zhangsun, and J. Wang, "Joint optical performance monitoring and modulation format/bit–rate identification by CNN–based multi–task learning," *IEEE Photon. J.*, vol. 10, no. 5, pp. 1–12, Oct. 2018.

[3] L. Guesmi, A. M. Ragheb, H. Fathallah, and M. Menif, "Experimental demonstration of simultaneous modulation format/symbol rate identification and optical performance monitoring for coherent optical systems," *J. Lightw. Technol.*, vol. 36, no. 11, pp. 2230–2239, Jun. 1, 2018.

[4] G. Yin, S. Cui, C. Ke, and D. Liu, "Reference optical spectrum based in–band OSNR monitoring method for EDFA amplified multispan optical fiber transmission system with cascaded filtering effect," *IEEE Photon. J.*, vol. 10, no. 3, Jun. 2018, Art. no. 7201910.

[5] H. Xu, "Joint scheme of dynamic polarization demultiplexing and PMD compensation up to second-order for flexible receivers," *IEEE Photon. J.*, vol. 9, no. 6, Dec. 2017, Art. no. 7204615.

[6] M. Wang and S. Wang, "An optical performance monitoring model based on RBFANN trained with eye–diagram," *Procedia Eng.*, vol. 29, pp. 53–57, 2012.

[7] F. N. Khan, K. Zhong, W. H. Al-Arashi, C. Yu, C. Lu, and A. P. T. Lau, "Modulation format identification in coherent receivers using deep machine learning," *IEEE Photon. Technol. Lett.*, vol. 28, no. 17, pp. 1886–1889, Sep. 1, 2016.

[8] C. Zhendong, J. Weining, X. Changbo, and L. Min, "Modulation recognition based on constellation diagram for M-QAM signals," in *Proc. IEEE 11th Int. Conf. Electron. Meas. Instrum.*, Aug. 2013, pp. 70–74.

[9] R. Borkowski, D. Zibar, A. Caballero, V. Arlunno, and I. T. Monroy, "Stokes space–based optical modulation format recognition for digital coherent receivers," *IEEE Photon. Technol. Lett.*, vol. 25, no. 21, pp. 2129–2132, Nov. 1, 2013.

[10] P. Chen, J. Liu, X. Wu, K. Zhong, and X. Mai, "Subtraction-clustering-based modulation format identification in Stokes space," *IEEE Photon. Technol. Lett.*, vol. 29, no. 17, pp. 1439–1442, Sep. 1, 2017.

[11] G. Liu, R. Proietti, K. Zhang, H. Lu, and S. J. Ben Yoo, "Blind modulation format identification using nonlinear power transformation," *Opt. Express*, vol. 25, no. 25, Dec. 2017, Art. no. 30895.

[12] F. N. Khan, K. Zhong, X. Zhou, W. H. Al-Arashi, C. Yu, C. Lu, and A. P. T. Lau, "Joint OSNR monitoring and modulation format identification in digital coherent receivers using deep neural networks," *Opt. Express*, vol. 25, no. 15, Jul. 2017, Art. no. 17767.

[13] W. Zhang, J. Kou, and Z. Wang, "Nonlinear aerodynamic reduced–order model for limit–cycle oscillation and flutter," *AIAA J.*, vol. 54, no. 10, pp. 3304–3311, Oct. 2016.

[14] J. Kou, W. Zhang, and M. Yin, "Novel wiener models with a time-delayed nonlinear block and their identification," *Nonlinear Dyn.*, vol. 85, no. 4, pp. 2389–2404, Sep. 2016.

[15] Y. Zhou, T. Anderson, K. Clarke, A. Nirmalathas, and K. Lee, "Bit-rate identification using asynchronous delayed sampling," *IEEE Photon. Technol. Lett.*, vol. 21, no. 13, pp. 893–895, Jul. 1, 2009.

[16] C. Sheng, J. Shang, X. Wenjuan, K. Changjian, and L. Deming, "Improved symbol rate identification method for on–off keying and advanced modulation format signals based on asynchronous delayed sampling," *Opt. Commun.*, vol. 354, pp. 218–224, Nov. 2015.

[17] B. Kozicki, O. Takuya, and T. Hidehiko, "Optical performance monitoring of phase-modulated signals using asynchronous amplitude histogram analysis," *J. Lightw. Technol.*, vol. 26, no. 10, pp. 1353–1361, May 15, 2008.

[18] H. Y. Choi, Y. Takushima, and Y. C. Chung, "OSNR monitoring technique for PDM-QPSK signals based on asynchronous delay-tap sampling technique," in *Proc. Nat. Fiber Optic Eng. Conf.*, 2010.

[19] F. N. Khan, A. P. T. Lau, T. B. Anderson, J. C. Li, C. Lu, and P. K. A. Wai, "Simultaneous and independent OSNR and chromatic dispersion monitoring using empirical moments of asynchronously sampled signal amplitudes," *IEEE Photon. J.*, vol. 4, no. 5, pp. 1340–1350, Oct. 2012.

[20] Y. Chen, G. Yu, Y. Long, J. Teng, X. You, B.-Q. Liao, and H. Lin, "Application of radial basis function artificial neural network to quantify interfacial energies related to membrane fouling in a membrane bioreactor," *Bioresource Technol.*, vol. 293, Dec. 2019, Art. no. 122103.

[21] Z. Zhao, Y. Lou, Y. Chen, H. Lin, R. Li, and G. Yu, "Prediction of interfacial interactions related with membrane fouling in a membrane bioreactor based on radial basis function artificial neural network (ANN)," *Bioresource Technol.*, vol. 282, pp. 262–268, Jun. 2019.
[22] E. Agrell and M. Karlsson, "Power–efficient modulation formats in coherent transmission systems," *J. Lightw. Technol.*, vol. 27, no. 22, pp. 5115–5126, Nov. 15, 2009.
[23] P. Winzer, A. Gnauck, C. Doerr, M. Magarini, and L. Buhl, "Spectrally efficient long-haul optical networking using 112-Gb/s polarization–multiplexed 16-QAM," *J. Lightw. Technol.*, vol. 28, no. 4, pp. 547–556, Feb. 15, 2010.

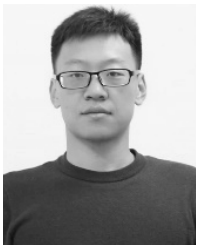

SIDA LI was born in Baoding, China, in 1995. He received the B.S. degree in intelligent science from the National University of Defense Technology, Changsha, China, in 2017. He is currently pursuing the Ph.D. degree in instrument science and technology with the Cyberspace Laboratory. His research interests include design and realization of coherent/non-coherent light demodulation systems, modulation formats identification, and signal features extraction for optical transmission networks.

JING ZHOU received the Ph.D. degree in instrument science and technology from the National University of Defense Technology, Changsha, China, in 2004. He is currently a Lecturer with the Cyberspace Laboratory, College of Intelligent Science, NUDT. His main research interests include cyberspace intelligent monitoring and signal processing for optical transmission networks.

ZHIPING HUANG received the Ph.D. degree in instrument science and technology from the National University of Defense Technology, Changsha, China. He has been a Professor with the Cyberspace Laboratory for several years. His research interests include cyberspace intelligent monitoring and signal processing for optical transmission networks.

XIAOYONG SUN received the B.S. degree from the Hebei University of Technology, Tianjin, in 2013, and the M.S. degree in instrument Science and technology from the National University of Defense Technology, Changsha, China, in 2017. He is currently pursuing the Ph.D. degree in instrument science and technology with the Cyberspace Laboratory. His research interests include modulation formats identification and signal features extraction for optical transmission network and cognitive radio.